Challenges and promises of lithium metal anode by soluble polysulfides in practical lithium–sulfur batteries

Li-Peng Hou [1], **Xue-Qiang Zhang** [1], **Bo-Quan Li**, **Qiang Zhang** *

Beijing Key Laboratory of Green Chemical Reaction Engineering and Technology, Department of Chemical Engineering, Tsinghua University, Beijing 100084, China

The lithium–sulfur (Li–S) battery has raised great expectations as a next-generation high-energy-density energy storage system. The multielectron dissolution–precipitation redox conversion of S affords a great contribution to its high specific energy. Spontaneously, the highly reactive Li metal anode always confronts soluble Li polysulfides (LiPSs) in a working Li–S battery, and parasitically side reactions occur inevitably. The challenges of the Li metal anode induced by soluble LiPSs emerge as roadblocks for practical Li–S batteries with the development of the S cathode from its infancy into growth stage. Therefore, the fundamental understanding of Li anode in the electrolyte with LiPSs and the targeted protection strategies are urgently required. In this review, the challenges of the Li metal anode in the presence of LiPSs are systematically analyzed. Then, the preliminary advances in Li metal anode protection to deal with LiPSs are summarized. Finally, an insightful outlook is put forward through both a fundamental understanding and a practical exploration of the Li metal anode to promote the development of practical Li–S batteries.

Keywords: Anode protection; Lithium-sulfur batteries; Polysulfides; Solid electrolyte interphase; Electrolyte

Introduction

In pursuit of a wireless, environment-friendly, and sustainable society, high-energy-density rechargeable batteries are highly required [1,2]. The lithium–sulfur (Li–S) battery with an estimated practical specific energy of over 500 Wh kg^{-1} has attracted intensive attention with the aim of bypassing the energy density ceiling of the current Li-ion batteries [3,4]. Nevertheless, Li–S batteries have undergone a tortuous developing road (Fig. 1). The prototype of Li–S batteries employing pure S as the cathode active material was firstly proposed by Herbet and Ulam in 1962 [5]. In the following four decades, a rechargeable high-performance S cathode was mainly hindered by the insulating nature of S and the shuttle effect of Li polysulfides (LiPSs) in working batteries [6–8]. Until the early 2000s, conductive carbon or polymer additives were added to construct a composite S cathode, enhancing the utilization of active S. The composite S/porous carbon cathode was demonstrated in 2002 by Wang et al.with an improved cyclability of the S cathode [6]. In 2009, a breakthrough in composite S/mesoporous carbon (S/C, carbon: CMK-3) cathode was proposed by Nazar and co-workers through a facile melt-diffusion strategy [9]. A high specific capacity of 1320 mAh g^{-1} (*ca.* 80% utilization based on active S) and decent cyclability were achieved.

However, the intrinsic challenges, including the insulative nature of S/Li_2S, the huge volume change (~80%) between S and Li_2S, and the shuttle effect of LiPSs, still hinder the S/C composite cathode. Therefore, remarkable progress has been made to further explore the composite S/C cathode and address its intrinsic shortcomings toward practical applications, such as optimization of carbon materials, design of cathode structure, and employment of catalyst to promote conversion kinetics, which are all regarded as important parts of regulations of S/C cathode. Various types of S cathodes, such as competitive sulfurized polyacrylonitrile, keep in pace along with the exploitation of

---

* Corresponding author.

E-mail address: Zhang, Q. (zhang-qiang@mails.tsinghua.edu.cn)

[1] These authors contributed equally to this work.

https://doi.org/10.1016/j.mattod.2020.10.021

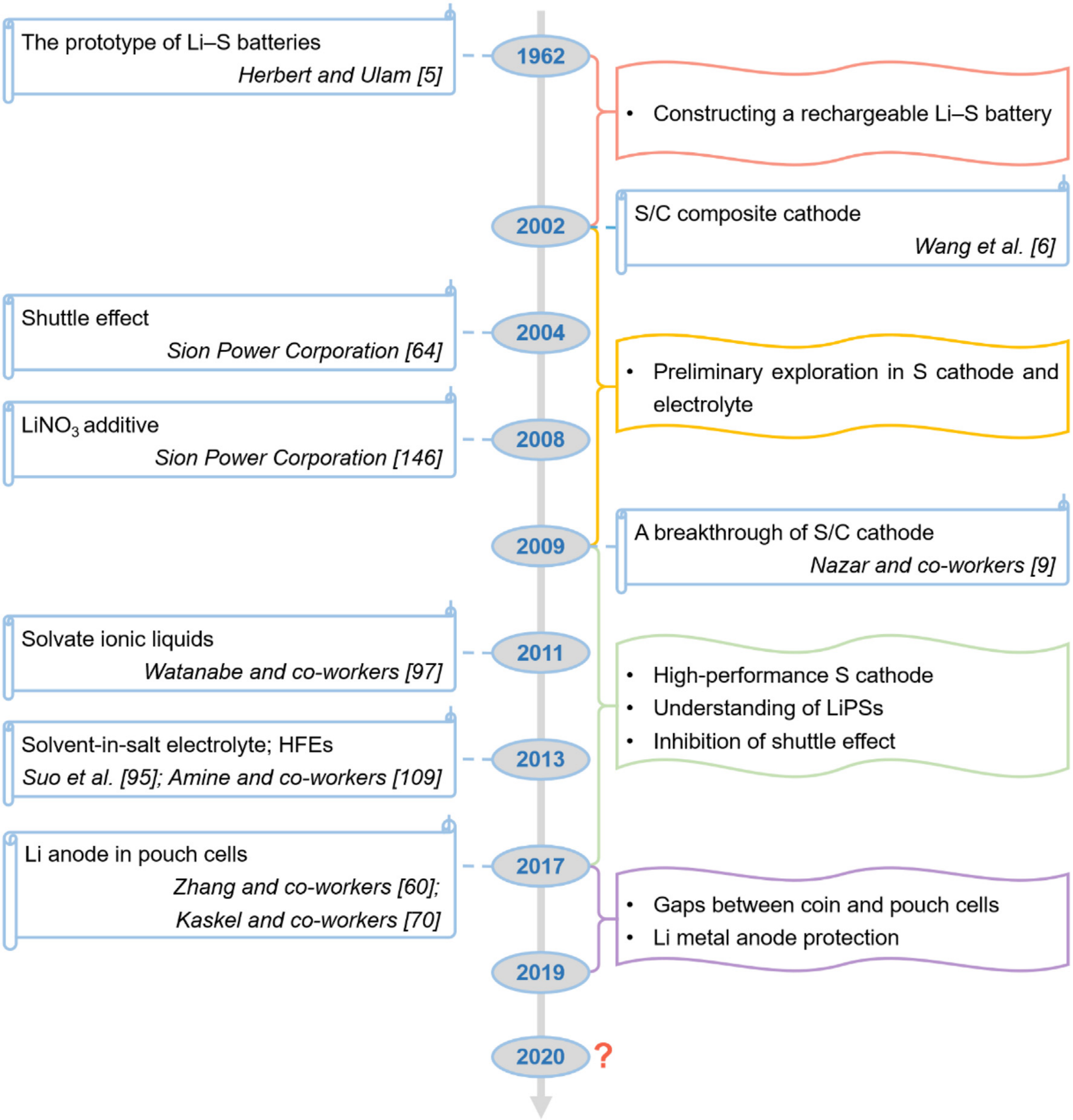

FIGURE 1

A brief summary of the development of Li–S batteries.

high-performance S/C composite cathode. However, in the race to develop practical Li–S batteries with a high energy density (>500 Wh kg^{-1}), composite S/C cathode is strongly considered owing to its high specific capacity, high discharge voltage, and facile scale-up [10–14]. Therefore, Li–S batteries which have experienced significant progress in regulations of cathode structure, conductive carbon materials, and electrochemical kinetics are focused on in this review. Despite the movement of the composite S/C cathode from its infancy into the growth stage in the past decade, the practical application of Li–S batteries is hindered by the new roadblocks of the Li metal anode [15–18].

In a typical Li–S battery with a composite S/C cathode, the active S undergoes a dissolution–precipitation redox conversion during discharge/charge. The initial reduction of S generates soluble LiPSs (*e.g.*, Li_2S_x, $4 \leq x \leq 8$) dissolving from carbon hosts into electrolyte. The further reduction of the soluble LiPSs results in the precipitation of Li_2S_2/Li_2S [19–21]. LiPSs inevitably shuttle between cathode and anode owing to concentration gradients or electromigration even though they promote S/Li_2S conversion for the high specific capacity (to some extent) as redox mediators. Polymer and solid-state electrolytes can effectively inhibit the formation of soluble LiPSs, yet their applications in practical Li–S batteries are in the preliminary stage and are not involved in this review. In a working Li–S battery with liquid electrolytes, Li anode is always confronted with vast reactive LiPSs.

Li is highly reactive and can react with most electrolytes which are composed of solvents, Li salts, and additives. The soluble LiPSs in electrolyte can be regarded as various solutes, which are in the oxidation state and easily reduced by chemical or electrochemical reactions with Li anode. Consequently, active LiPSs and fresh Li are depleted by side reactions. The loss of active materials induces the rapid decay of batteries. Moreover, the behaviors of Li deposition and stripping are strongly dictated by the uniformity of solid electrolyte interphase (SEI). LiPSs involve in the formation and evolution of SEI, degenerating the subsequent uniformity of Li plating/stripping and the final stability of a Li–S battery. Therefore, the challenges of the Li metal anode induced by soluble LiPSs must be taken into consideration in either a prototype or a practical Li–S battery.

Particularly, for a practical Li–S battery with high energy density, practical conditions of a high S loading (>5.0 mg cm^{-2}), a low electrolyte/sulfur (E/S) ratio (<3.0 μL mgs^{-1}), and a limited Li anode (<50 μm) are highly suggested [10–13]. On the contrary, mild conditions, including a low S loading (<2.0 mg cm^{-2}), a high E/S ratio (>10.0 μL mgs^{-1}), and an excessive Li anode (>500 μm), are employed to investigate the fundamental physicochemical features of Li–S batteries in most reports. According to theoretical calculations, a concentration of soluble LiPSs (>6.0 M [S] species) is produced in electrolyte under practical conditions, which is much higher than that under mild conditions. Therefore, the much-limited Li and lean electrolyte can be depleted rapidly, irreversibly giving rise to a short lifespan of Li–S batteries. Disclosing the gap of the influence of LiPSs on Li anode between mild and harsh conditions is necessary. Moreover, the challenges of the Li metal anode under practical conditions are critical for pushing forward the process of Li–S batteries and deserve further exploration [22,23].

In this review, the challenges and promises of the Li metal anode in practical Li–S batteries are presented. Firstly, the challenges of the Li metal anode confronting LiPS intermediates are analyzed, including the formation of soluble LiPSs in bulk electrolyte, the corrosion of LiPSs on Li anode, and the influence on SEI. The recent advances in Li metal anode protection in Li–S batteries are summarized, including the inhibition of LiPS dissolution, the reduction of LiPS activity, and the reinforcement of anode/electrolyte interphase and bulk Li. It should be noted that accelerating the conversion kinetics of LiPSs and employing functional interlayers to shield LiPSs are also effective approaches to indirectly decreasing the impact of LiPSs on Li metal anode, as summarized in recent impactive reviews [15–18,24,25], but these are beyond the scope of this review. Finally, an insightful outlook is presented to promote the fundamental understanding and practical applications of the Li metal anode in Li–S batteries.

The challenges of the Li metal anode in LiPS electrolyte

Soluble LiPSs must be considered within the fundamental properties and complicated entanglement with the Li anode in Li–S batteries compared to other Li metal batteries with Li-containing intercalation-type cathodes [26–31] such as $LiCoO_2$, $LiFePO_4$, and $LiNi_xCo_yMn_{1-x-y}O_2$ (Fig. 2, Table 1), but they are seldom discussed in most previous reports. First, LiPSs dissolve into electrolyte once the electrochemical reaction occurs, inducing new components in electrolyte and altering the original electrolyte structure. Second, Li metal corrosion is aggravated due to the exposed fresh Li in LiPS electrolyte or the permeation of LiPSs through SEI. Third, a multicomponent SEI consisting of Li_2S/Li_2S_2 is formed by the reaction between LiPSs and Li anode, which may interfere with the transport of Li ions and then change the Li morphology.

LiPSs in bulk electrolyte

Polysulfides, dianions (*e.g.*, S_4^{2-}, S_6^{2-}, and S_8^{2-}), and radical monoanions (*e.g.*, $S_3^{\cdot-}$) can coexist in electrolyte. The dianions of S_4^{2-}, S_6^{2-}, and S_8^{2-} are stable in low donor number solvents, such as tetrahydrofuran (THF), 1,3-dioxolanne (DOL), and 1,2-dimethoxyethane (DME), while $S_3^{\cdot-}$ radical is the main intermediate in high donor number solvents, such as dimethyl sulfoxide (DMSO), dimethylformamide (DMF), dimethylacetamide (DMA), and tetramethylurea (TMU) [32–35]. Solvents with a high number of solvating oxygen atoms but low donor number and dielectric constant, such as tetra ethylene glycol dimethyl ether (TEGDME), show an equalized coexistence of free radicals and dianions [34,36–38]. Still, the applicable solvents for rechargeable Li–S batteries are very limited due to the nucleophilicity of LiPSs [39,40].

DOL and DME are the most common solvents in Li–S batteries and cause LiPSs to suffer a solid–liquid–solid conversion with different configurations (Fig. 3a) [19–21]. In addition to the dynamic configurations mentioned, the concentration of LiPSs fluctuates significantly during the discharge/charge process. Under practical applications, the lean electrolyte but vast active S results in a high concentration of LiPSs [10–13]. For instance, the theoretically maximal concentration of LiPSs can be up to 10.4 M [S] at an E/S ratio of 3.0 μL mgs^{-1} if active S delivers a specific capacity of 1672 mAh g^{-1} (Fig. 3a), ignoring the volume change during the dissolution of LiPSs. Additionally, with the solid–liquid–solid conversion, the concentration of LiPSs changes drastically, sharply increasing to 10.4 and decreasing to 0.0 M [S]. Specifically, it should be noted that the calculation is based on a theoretical case, while the practical situation is influenced by the actual solubility and disproportionation reaction of LiPSs, the dissolving power of solvents, the utilization degree of active S, and so on.

The properties of the electrolyte also change with the additional and dynamic LiPSs compared with the typical Li metal batteries with intercalation-type cathodes. In a practical Li–S battery, the concentration of the dissolved LiPSs increases with the increase of S utilization and the reduction of E/S ratio (Fig. 3b). A high-concentration S electrolyte is formed with the soluble LiPSs beyond 4.0 M [S] if LiPSs completely dissociate based on Li_2S_8. The dissolution of LiPSs inevitably increases the viscosity of electrolytes [41–43]. A concentration of 5.0 M [S] LiPSs in TEGDME renders a 4-time rise on the viscosity of electrolyte [41]. Moreover, the ionic conductivity generally reduces when the Li ion concentration is over 1.0 M [42]. Furthermore, the theoretical concentration of LiPSs possibly exceeds the dissolution capability of electrolytes, inducing a saturated LiPS solution. For instance, the solubility of LiPSs is *ca.* 6.0 M [S] in the routine electrolyte based on DOL/DME (1:1, by vol.) [44,45], which is less than the theoretically maximal LiPS concentration of 10.4 M [S] when the E/S ratio is below 3.0 μL mgs^{-1}. The saturation of LiPSs can change the discharge/charge mechanism. The original liquid–liquid (Li_2S_x, $x \geq 4$) and liquid–solid (Li_2S_4 to Li_2S_2/Li_2S) conversion zones will then be shifted to solid–solid conversion; that is, high-order LiPSs will be saturated and precipitated [46,47]. For example, at the end of the first discharge platform, Li_2S_4 with a low solubility easily reaches saturation. A large

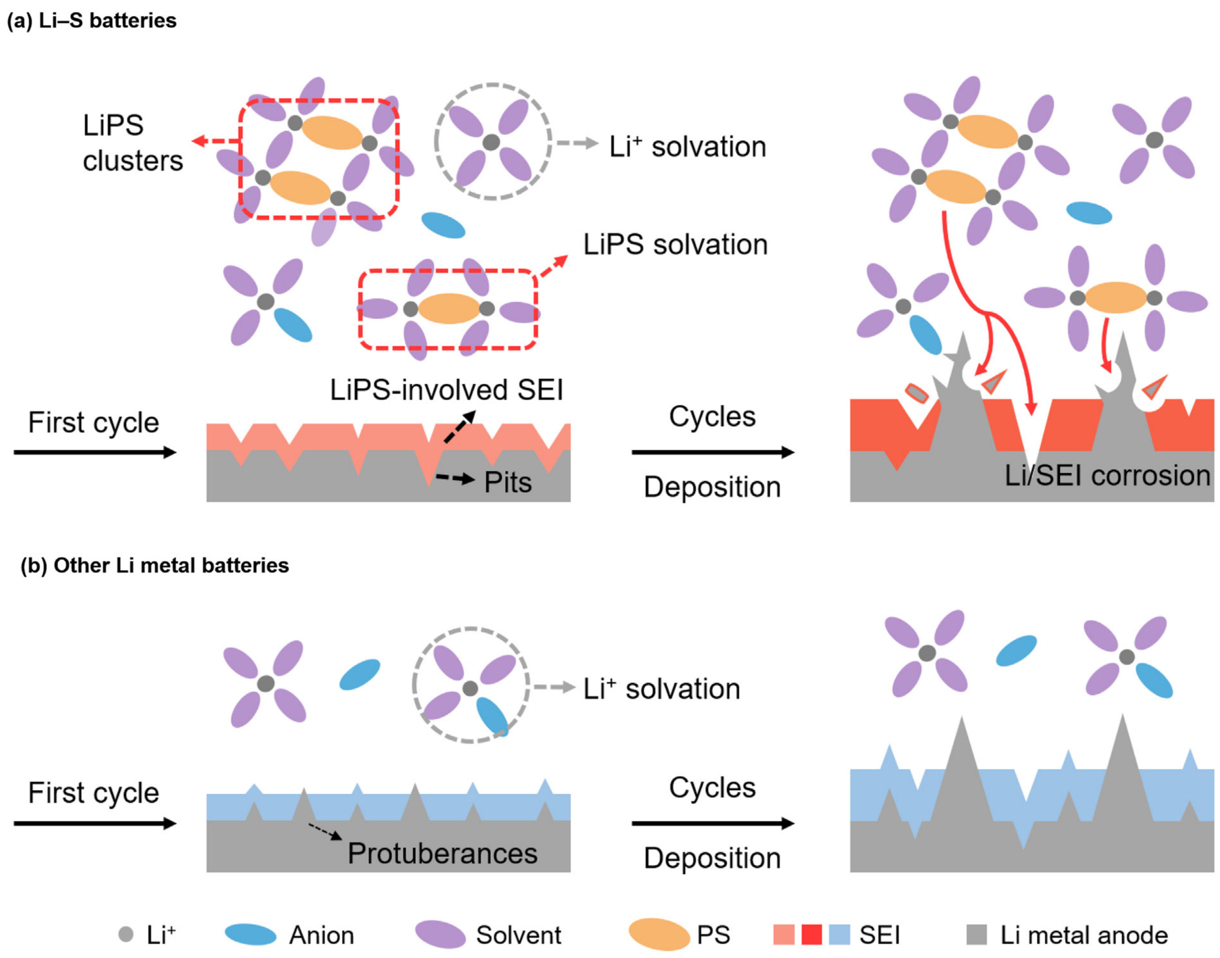

FIGURE 2

The comparison of a working Li metal anode in Li–S batteries and other Li metal batteries. The evolution of the Li metal anode in (a) Li–S batteries with the soluble LiPS intermediates and (b) other Li metal batteries employing intercalation-type cathodes without LiPSs.

TABLE 1

The differences in the challenges of Li metal anode in Li–S batteries and Li metal batteries with intercalation-type cathodes.

	Li–S batteries	**Li metal batteries with intercalation-type cathodes**
Electrolyte	a) Soluble LiPSs b) The partial or complete dissociation of LiPSs to impact the solvation of Li ions c) Concentrated and dynamic LiPSs in electrolyte	No LiPSs
Li metal anode	a) Li stripping firstly b) The corrosion of LiPSs on Li	Li plating firstly
SEI	a) The involvement of LiPSs into the formation of SEI b) The penetration of LiPSs in SEI	No LiPSs

nucleation resistance appears with an apparent voltage dip in a discharge profile [48]. With LiPSs gradually converting to solid Li_2S_2/Li_2S, the corresponding discharge polarization recovers. During charging, a similar solid Li_2S–liquid LiPSs (Li_2S_{4-8})–solid S_8 conversion occurs, which means that a high concentration of soluble LiPSs at the mid-state of charge is also inevitable. However, the conversion mechanism during the charge at a low E/S ratio is significantly lacking. Moreover, the component distribution of LiPSs changes with the electrolyte composition (solvents, Li salts, *etc.*). For example, in solvents with a high donor number, such as DMSO, there is a chemical balance between S_6^{2-} and $S_3^{\cdot-}$ instead of the dominant electrochemical balance among S_8^{2-}, S_6^{2-}, and S_4^{2-} [44]. Specifically, the chemical balance between S_6^{2-} and $S_3^{\cdot-}$ ($S_6^{2-} \rightarrow 2S_3^{\cdot-}$) at a low E/S ratio changes sharply to the left compared to that at a high E/S ratio. Therefore, the complicated existence and conversion of LiPSs increase the difficulty of protecting the Li anode in Li–S batteries under practical conditions.

To provide a precise forecast of the electrolyte with LiPSs, the basic physicochemical parameters of LiPSs are vital. There are two main processes for LiPSs entering electrolyte, including dissolution and dissociation. Firstly, a LiPS can dissolve in elec-

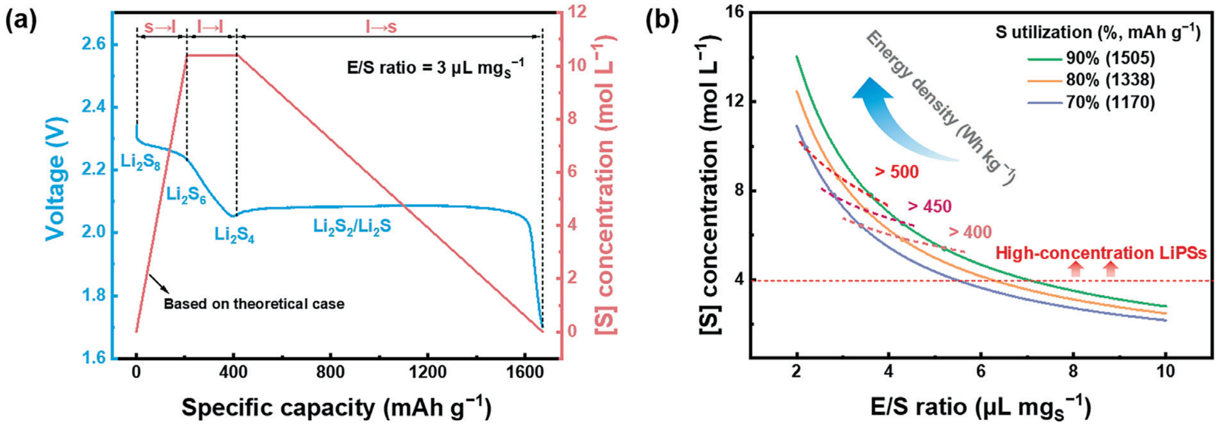

FIGURE 3

Calculations of the evolution of LiPSs. (a) Typical discharge profile of Li–S batteries and the concentration evolution of total S species based on a low E/S ratio of 3.0 μL mgs^{-1}. (b) The concentration of soluble LiPSs under various E/S ratios and S utilizations.

trolyte as a neutral molecule (*e.g.*, Li_2S_x); then, the neutral Li_2S_x can dissociate to one or two Li ions and form LiS_x^- or S_x^{2-} through solvation. Dissolution occurs when a solute disperses in a solvent to form a homogeneous solution [49,50]. The maximal dissolution capability is defined as solubility. Generally, the Li^+–S_x^{2-} pair binding is stronger in low-order LiPSs than that in high-order ones. Therefore, the solubility and dissociation degree of LiPSs in electrolyte have a positive correlation with the chain length of polysulfides. The low dissociation degree of low-order LiPSs contributes to a low ionic conductivity (~1.0 mS cm^{-1} of Li_2S_4 and ~3.0 mS cm^{-1} of Li_2S_8 based on 0.5 M LiPSs in DOL/DME) [43]. Moreover, the diffusion coefficient of high-order polysulfides (S_6^{2-} and S_8^{2-}) is lower than that of low-order ones (S_4^{2-}) due to the particle's effective size according to Stokes-Einstein relations (~3.0×10^{-10} and 5.0×10^{-10} m^2 s^{-1} of S_8^{2-} and S_4^{2-}, respectively, based on 0.25 M LiPSs in DOL/DME) [43,51]. If LiPSs do not dissociate or even combine with Li ions to form cations ($Li_3S_x^+$), the diffusion and electromigration will be more complex. LiPSs also readily aggregate into clusters, namely $(Li_2S_x)_n$. Low-order LiPSs tend to form larger clusters compared to high-order ones, which is ascribed to the stronger charge localization at the terminal S atom [43,52]. Therefore, the dynamic LiPSs with complicated properties, such as solubility, ionicity, diffusion coefficient, and reactive activity, have a vital impact on the properties of bulk electrolyte which the Li metal anode confronts.

The corrosion of LiPSs on the Li metal anode

The corrosion of LiPSs on the Li metal anode was recorded experimentally in the early 1980s [53,54]. There are three main factors related to the corrosion reaction, including the species of LiPSs (reactive activity), the concentration of LiPSs, and the exposed active surface of Li metal. First, LiPSs are oxidative while Li metal has strong reducibility. The oxidizing ability of LiPSs is positively correlated with the length of the polysulfide chain. In other words, the activity of high-order LiPSs is higher than that of low-order ones [55]. In a routine electrolyte composed of DOL/DME and LiTFSI, high-order LiPSs, such as Li_2S_8 (ring or linear), tend to preferentially react with Li metal compared with LiTFSI and DOL/DME solvents due to an advantage in Gibbs free energy change [55,56]. The dissolved trace S element in electrolyte can accelerate the corrosion [54]. Secondly, the high concentration of LiPSs produced at the cathode will generate a large concentration gradient at a low E/S ratio and a high S loading, which accelerates the chemical diffusion of LiPSs and may induce raging corrosion on Li metal [57,58]. Thirdly, Li deposition is dendritic or whiskered. The contact area between Li and electrolyte rapidly increases after repeated cycles compared with the original plane. When the SEI is cracked owing to the huge volume change, fresh Li exposes to LiPS electrolyte. The huge active surface area exacerbates the erosion reaction. The spatially inhomogeneous deposition of Li owing to the increased electrode area is also considered in a pouch cell [59–61].

The corrosion of LiPSs on Li metal causes a series of issues. High-order LiPSs produced at the cathode can diffuse to the anode and react with exposed fresh Li metal, thus forming solid Li_2S/Li_2S_2 and soluble low-order LiPSs [62]. The accumulative low-order LiPSs diffuse back to the cathode, which is known as the shuttle effect [63,64]. Furthermore, the corrosion of LiPSs on Li metal also gets involved in the Li morphology. The deposited Li is etched during plating, which induces the dissolution of flimsy segments. The plated Li loses the connection to the electrode and forms dead Li [65]. Further, mossy Li is aggravated in the presence of LiPSs [66]. Mossy Li not only increases the exposed active surface in electrolyte and exacerbates the corrosion, but also raises the risk of the pulverization of the Li anode, leading to increased internal resistance and the final failure of batteries. Furthermore, safety concerns caused by Li dendrite growth should be paid extreme attention to in pouch cells. The propagation of the Li dendrite due to the local inhomogeneous current density, huge utilization of the Li anode during each plating/stripping, and unstable SEI during the long-term cycling not only exacerbates the electrolyte depletion and Li powdering, but may also pierce the separator and cause a short circuit. Particularly, it should be noted that various patterns of non-uniform Li deposition are simplistically overgeneralized as "Li dendrites", such as whiskered, needlelike, and mossy Li [67]. However, the distinctive mechanisms may be behind the different morphologies of Li deposition, and therefore the corresponding name of the morphology should be specific. Additionally, the continuous parasitic reactions between the Li anode and the electrolyte will result in another safety hazard, namely a gassing problem. The reduction of solvents (DOL/DME) produces CH_4 and H_2 [68,69]. Even if the functional additive $LiNO_3$ is utilized, gassing still exists in Li–S pouch cells [70] and requires more investigation.

The impact of LiPSs on SEI

The Li metal anode can react with nearly all electrolyte components to form SEI, and SEI is usually multicomponent and spatially heterogeneous. The components and structure of SEI are directly related to the electrolyte recipes [71]. In Li–S batteries, the decomposition products of LiPSs can also become the ingredients of SEI, further affecting the subsequent behaviors of Li utilization [72,73]. Besides, the reactive LiPSs can permeate through the formed SEI or even react with specific components in SEI, which complicates the understanding and regulation of SEI [55,62].

Li_2S_2/Li_2S is usually enriched in the bottom layer of SEI near the surface of the Li anode due to the prior reaction between LiPSs and Li metal compared to solvents and Li salts [63,74]. Moreover, the content of Li_2S_2/Li_2S in the SEI rises with the increased concentration of LiPSs [75]. As aforementioned, LiPSs are diverse and dynamic during cycling, and thus the dynamic change of SEI in terms of components and structure is expected. For a pouch cell, an inhomogeneous spatial distribution of highly concentrated LiPSs is possible due to the large area of the electrode. Therefore, the distribution of Li_2S_2/Li_2S in the SEI may also be disordered, which further influences the cycle performance of the Li anode.

The changes in the SEI directly impact the behaviors of Li plating and stripping. In the SEI with Li_2S, the low ionic conductivity of Li_2S is usually insufficient for rapid Li ion transport and increases interfacial impendence. The stripping of Li easily starts from the defects of Li_2S passivation layer, forming irregular and discrete pits on the Li metal surface [76]. The pitting effect becomes serious with the increase of current density. During the following charge process, LiPSs prefer to corroding the vimineous Li dendrites, thus forming mossy Li [65,66]. Meanwhile, the freshly formed SEI on the bumpy surface with a large specific surface area is too thin to shield the permeation and erosion of LiPSs on new plated Li, thus accelerating the depletion of electrolyte and active Li. Furthermore, Li–S batteries start from discharge during cycling, that is Li strips first. The utilization patterns of Li are relative to the order of initial Li plating or stripping [77,78], and the presence of LiPSs can deteriorate the utilization of the Li anode.

The influence of LiPSs on the erosion of SEI components through the strong intermolecular interaction is also vital, which will cause the rapid fracture of SEI. Murugesan and co-workers demonstrated that the LiPSs in electrolyte near the Li metal surface can be entrapped by the fluorine-/sulfur-containing species in the initial SEI because of a strong interaction between LiPSs and the polar species in SEI [79]. It is a universal strategy to employ the interaction between polar molecules and LiPSs to promote the electrochemical conversion of LiPSs at composite cathodes [80], such as chemical adsorption[81–83] and electrocatalysis [84–86]. Similarly, LiPSs may be recruited by the partial SEI ingredients indeed. The reaction between the S element and Li_2O, the most common SEI component, has been testified in the electrolyte with the assistance of trace moisture by high-performance liquid chromatography analysis [87]. However, more investigations are required to disclose the impact of LiPSs on SEI evolution for further rational design on Li metal anode protection.

The working Li metal anode in Li–S batteries

Specific protective requirements for the Li metal anode are required in Li–S batteries compared to other Li metal batteries. The protection strategies for the Li anode in Li metal batteries with intercalation-type cathodes have been summarized in previous reviews [88–91] and are not presented in this review. There are mainly three aspects to protect the Li metal anode in Li–S batteries considering that the origin of LiPSs is from the redox of S/Li_2S at the cathode side. Firstly, inhibiting LiPS dissolution is a fundamental way to minimize the crosstalk between the cathode and Li anode. Secondly, stabilizing LiPSs through regulating the solvation structure can decrease LiPS activity to weaken the corrosion on the Li metal anode. Thirdly, optimizing the SEI or reinforcing the bulk Li metal also can protect the Li anode even if there are dissolved LiPSs.

Inhibiting the dissolution of LiPSs

Decreasing LiPSs in the electrolyte can slow down the corrosion on the Li anode. The solubility of LiPSs greatly associates with solvents. When the intermolecular force between solvents and LiPSs (*e.g.*, Van der Waals forces) is stronger than the cohesion of LiPSs, the dissolution of LiPSs tends to occur. The lower the number of free solvent molecules in the electrolyte, the lower the absolute amount of LiPSs dissolved. Therefore, turning the solvation structure by reducing free solvents or employing low polar solvents can sparingly dissolve LiPSs (Fig. 4).

The concentration of Li salts impacts the dissolution of LiPSs. The solvent molecules in electrolyte partially participate in the solvation sheaths of Li ions, and the other parts move freely without coordination. The free solvent is one of the reasons for the dissolution of LiPSs (Fig. 4a). It has been demonstrated that increasing the concentration of Li salts can decrease the free solvents to inhibit LiPS dissolution [92–94]. A new class of “solvent-in-salt” electrolyte for Li–S batteries was proposed by Hu and co-workers [95]. The ultrahigh salt concentration (7 M LiTFSI in DOL/DME) decreases the soluble LiPSs and promotes smooth Li deposition. Nazar and co-workers further illustrated that a reinforced three-dimensional electrolyte network is established through each $TFSI^-$ binding with multiple Li ions in the electrolyte which consists of diethylene glycol dimethyl ether (G2) and LiTFSI (0.8:1, by mol) [96]. The solubility of Li_2S_6 is only 0.44 mg mL^{-1} ($\sim$2.0 mM Li_2S_6) at room temperature, and the activity of the whole electrolyte is weakened toward Li metal, inducing uniform Li deposition. When the glyme and LiTFSI are equimolar, triglyme (G3) or tetraglyme (G4) tends to form glyme–Li salt molten complexes like $[Li(G3\ or\ G4)_1][TFSI]$. The glyme molecules coordinate with Li ions to form a whole large cation and few free solvents remain, which are called solvate ionic liquids [97,98]. The solubility of Li_2S_8 in $[Li(G3)_1][TFSI]$

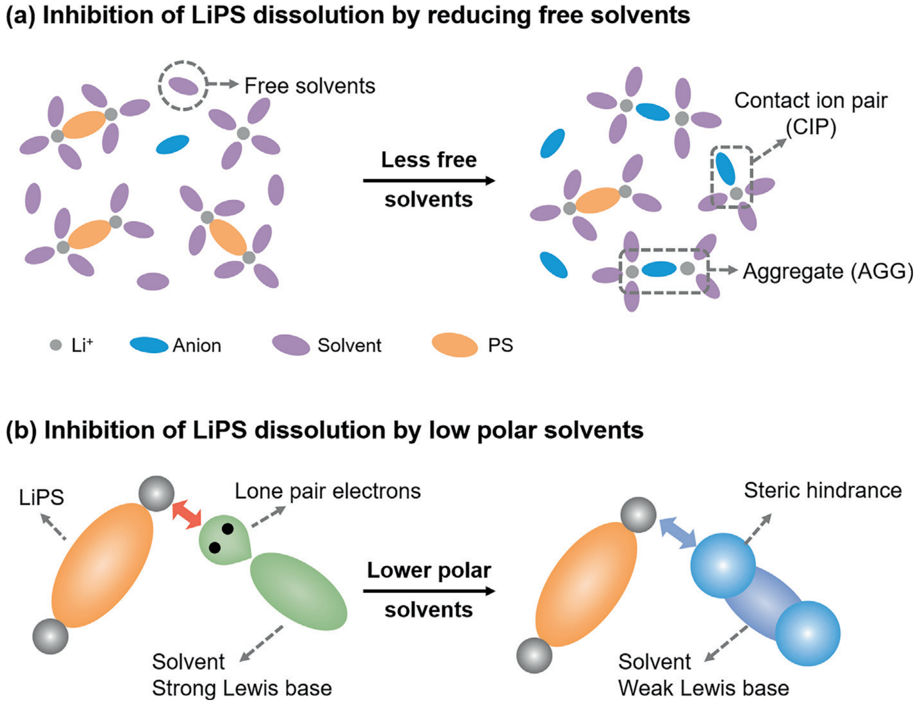

FIGURE 4

The strategies to inhibit LiPS dissolution. (a) Reducing free solvent molecules to achieve low LiPS solubility, which can be realized by highly concentrated electrolyte and solvate ionic liquids. (b) The introduction of low polar solvents with weak Lewis basicity or high steric hindrance to suppress LiPS dissolution. The solvents with a high C/O ratio or electron-withdrawing functional groups contribute to low polarity.

and $[Li(G4)_1][TFSI]$ is *ca.* 29 and 62 mM (based on total [S]), respectively [98]. However, neither highly concentrated electrolyte nor solvate ionic liquids can circumvent the high viscosity, resulting in a low Li ion conductivity ($\sim 10^{-3}$ S cm^{-1}, an order of magnitude lower than that of traditional dilute organic electrolytes). Consequently, the discharge voltage plateau is generally with a large hysteresis, which decreases the energy density of Li–S batteries. Recently, some publications demonstrated that lowering the concentration of Li salts also can inhibit the dissolution of LiPSs. A low concentration of salts below 0.3 M can not only suppress the dissolution of short-chain polysulfides, but can also improve the electrode wetting and rate capability [99,100]. The application potential of low salt concentration electrolyte in pouch cells needs to be further investigated.

The polarity of a solvent is another crucial factor that affects LiPS dissolution via the principle of similar compatibility (Fig. 4b). Dielectric constant ε_r, carbon/oxygen (C/O) ratio, and steric hindrance can simply reflect the polarity of a solvent. Ethers like DOL (C/O = 1.5, $\varepsilon_r = 7.30$) and DME (C/O = 2, $\varepsilon_r = 7.20$) exhibit a high solubility of LiPSs due to the strong electrostatic interactions between O atoms and Li ions. Homologous ethers with high C/O ratios are usually highly nonpolar, enabling a low LiPS solubility [101,102]. For example, diisopropyl ether (DIPE) with a C/O ratio of 6 and high steric hindrance has a lower LiPS solubility compared to dipropyl ether (DPE), methyl tert-butyl ether (MTBE), and methyl butyl ether (MBE) [101]. The DIPE/DOL/DME (50:25:25, by vol.) electrolyte with a LiPS solubility of ~ 0.1 M Li_2S_8 reduces the percentage of sulfur-containing species on the Li anode surface and alleviates the shuttle effect. Further, the superior properties of ethers maintain, *e.g.*, good compatibility with Li metal, appropriate solubility of Li salts, and low viscosity.

Furthermore, introducing highly electron-withdrawing groups into solvent molecules can reduce the Lewis basicity (Fig. 4b). Relatively non-polar *N,N*-dimethyl triflamide (DMT) and *N,N*-dipropyl triflimide (DPT) have been employed in Li–S batteries to achieve a sparing solubility of LiPSs [103]. Hydrofluoroethers (HFEs) possess abundant fluorine atoms with strong electro-negativity and electron-withdrawing effect, displaying a low affinity to Li ions to suppress the dissolution of LiPSs [104]. The structure of HFEs determines the solvation ability, including the degree of fluorination and the position of fluoroalkyl groups [105–107]. Generally, the higher degree of fluorination there is, the lower coordination capability to Li ions the HFEs will have [108]. Amine and co-workers further demonstrated that the position of fluorine atoms is more dominant than the number for the solvation [107]. HFEs with α- and β′-substituted fluoroalkyl groups usually exhibit the lowest solvating ability of Li ions.

Additionally, the viscosity of HFEs is low (generally <10 cP), enabling HFEs to be extensively employed as diluents into highly concentrated electrolyte, such as 1,1,2,2-tetra-fluoroethyl 2,2,3,3-tetrafluoropropyl ether (TTE) [96,109–112], bis(2,2,2-trifluoroethyl) ether (BTFE) [113,114], 1,1,2,2-tetrafluoroethyl 2,2,2-trifluoroethyl ether (TFTFE) [115,116], and 1H,1H,5H-octa fluoropentyl-1,1,2,2-tetrafluoroethyl ether (OFE) [117]. This electrolyte is named as localized high concentration electrolyte (LHCE) as Li salts are barely soluble in HFEs. LHCE combines the merits of a decreased amount of free solvent molecules and reduced polarity of solvent molecules. Not only are the viscosity and wettability ameliorative, but also the corrosion of LiPSs on Li metal is restrained. In a LHCE, almost all main solvent molecules participate in Li ion solvation to form contact ion pairs (CIP) and aggregates (AGG) with nearly no residual free solvent molecules (Fig. 4a). Therefore, solvents which are unstable with Li metal in a dilute electrolyte (*e.g.*, acetonitrile (ACN) and sulfolane (SL)) become relatively stable in LHCE [118–122].

The ionic liquid is composed of large cations and anions only, which is an alternative system to suppress the dissolution of LiPSs [49,70,123–125]. The dissolution of LiPSs in ionic liquids is related to the Lewis basicity and metathesis reaction. Donor number is a descriptor for basicity, which is positively correlated to the solubility of LiPSs [126,127]. If the size of the ionic LiPSs (*e.g.*, S_x^{2-}, LiS_x^-, $Li_3S_x^+$) and the ions of ionic liquids matches, site exchange may readily occur to facilitate the LiPS dissolution [127,128]. Among diversiform ionic liquids, $[TFSI]^-$ based ionic liquids prevail due to the weak coordination of $[TFSI]^-$ in inhibiting LiPS dissolution and excellent electrochemical properties [127,129]. However, the high viscosity and cost of ionic liquids are still obstacles for the applications in practical Li–S batteries [49]. Overall, the low solvation power of low polar solvents is a double-edged sword. The poor solubility of LiPSs in return delays the electrochemical kinetics of S/Li_2S conversion, which even alters the reaction pathway from a dissolution–precipitation to a quasi-solid-state or solid–solid conversion. Therefore, Li–S batteries involving low polar solvents generally exhibit a low charge/discharge rate and a large voltage hysteresis, which requires the assistance of the elevated working temperature.

Reducing LiPS activity

Reducing the reactive activity of LiPSs with Li metal is another consideration to protect the Li metal anode. The dissociated polysulfides (S_x^{2-}, $4 < x \leq 8$) are a series of Lewis bases [21]. Lewis acids, such as large cations of ionic liquids, can coordinate with and stabilize polysulfides by forming ion–ion complexes according to hard and soft acids and bases theory [130,131]. *N*-methyl-*N*-ethyl pyrrolidinium cation (MEP^+) thermodynamically prefers to forming stable MEP^+–S_x^{2-} complexes due to a low Gibbs free energy (Fig. 5a) [132]. The complexation not only improves the stability of high-order LiPSs that are highly reactive with Li metal but also changes the decomposition pathway of the electrolyte, inducing a low Li nucleation radius and low SEI impendence [132]. These discoveries provide fresh insights on the role of ionic liquids in Li–S batteries besides the general concept of low LiPS solubility [127,133–135]. Ionic liquids as additives instead of main solvents may alleviate the disadvantages, such as high viscosity, limited ion conductivity, and expensiveness.

The basicity of low-order LiPSs is stronger than that of high-order ones. Hence, relatively hard acids, such as alkali metal cations, are effective to stabilize low-order polysulfides. Rb^+ with weak solvation energy tends to coordinate with low-order LiPSs (*e.g.*, S_4^{2-}/S_3^{2-}) through the strong electrostatic interaction [136]. Ammonium salts (such as NH_4TFSI, NH_4I, and NH_4NO_3) are also used as additives to facilitate the stability of low-order polysulfides and even solid Li_2S due to the strong interaction between NH_4^+ and S_x^{2-} [137,138]. Reducing LiPS activity toward the Li anode is an emerging but crucial direction which requires in-depth exploration in the future.

LiPSs not only exist in the term of monomers (Li_2S_x) but also easily aggregate to clusters, namely $(Li_2S_x)_n$ [33,51,52,139]. The large clusters of Li_2S_4 increase the viscosity of electrolyte, giving rise to a sharp voltage drop during the second discharge plateau, which is even severe at low temperatures [51,140]. Although the influence of LiPS clusters on the stability of the Li metal anode is vague up to now, the role of Li salts in regulating the cluster behaviors of LiPSs is under investigation. LiTFSI can weaken the formation of clusters through electrostatic screening but with a limited effect [43,51]. Lithium trifluoroacetate (LiTFA) with similar ionic association energy to LiPSs can discourage clusters by the competitiveness of salt anions for Li ions (Fig. 5b) [140]. Lithium trifluoromethyl-4,5-dicyanoimidazole (LiTDI) enables Li_2S_4 to agglomerate into $(Li_2S_4)_2$ dimer due to the abundant nitrogen-containing functional groups [141]. Moreover, TDI^- with low mobility and weak interaction with LiPSs is in favor of suppressing the dissolution of LiPSs [142]. Therefore, a dense Li deposition is achieved [141].

However, decreasing the activity of LiPSs to protect the Li anode is a trade-off with the normal kinetic conversion of the cathode. Although parasitic reactions with the Li metal anode are alleviated by decreasing the reactivity of LiPSs, the reaction kinetics of LiPSs at the cathode can also simultaneously be suppressed. A compromise between protecting the Li metal anode and maintaining the kinetic performance of the cathode should be considered to achieve a practical high-energy-density Li–S battery. Therefore, the stabilization of LiPSs is a challenging work, and precise regulation is in demand for Li metal anode protection.

Reinforcing the anode/electrolyte interphase and bulk Li

The SEI is considered to be the main factor in dictating the flux of Li ions and the Li plating/stripping behaviors since it was proposed by Peled in 1979 [143]. However, SEI is generally fragile and spatially heterogeneous, leading to uncontrollable Li dendrites and low utilization of Li metal [72,73]. With regard to Li–S batteries, the formation of a robust SEI in the presence of LiPSs is necessary by either isolating or involving LiPSs from the formation of the SEI. Additionally, the basic requirements of SEI are also necessary, such as homogeneous Li ion diffusion channels, low interfacial resistance, and certain mechanical strength [144,145]. The artificial coating is a useful supplement to increase the stability of the anode/electrolyte interphase. Moreover, strengthening bulk Li metal is also a renewed approach to improve the adaptability of Li metal in LiPS electrolyte.

In situ SEI

SEI plays a vital role in alleviating the corrosion of LiPSs on the Li anode and in regulating Li deposition. The regulation of electrolyte components, such as solvents, Li salts, and additives, is a direct way to ameliorate the anode/electrolyte interphase through the spontaneous reaction with Li metal to form an *in situ* SEI.

$LiNO_3$ is regarded as an effective additive to protect Li metal by forming a stable SEI since it was proposed by Sion Power Corporation in 2008 [146]. $LiNO_3$ can be reduced by Li metal to form LiN_xO_y in the SEI, generating a compact passivation film to pro-

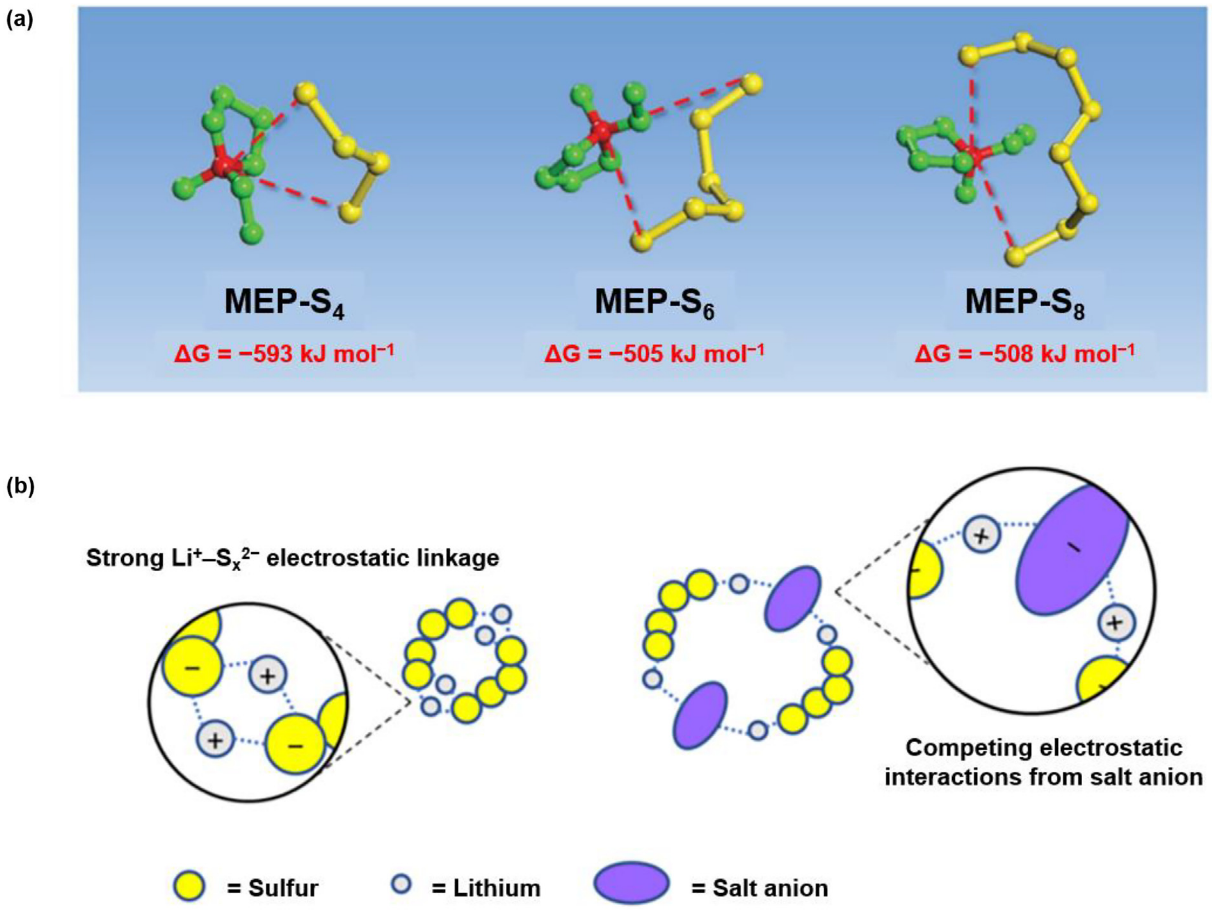

FIGURE 5

Stabilizing LiPSs to reduce the reactivity with a Li anode. (a) Product configuration and Gibbs free energy for the complexing reaction between MEP^+ and S_x^{2-}. (Reprinted with permission from [132], 2018, Wiley-VCH.) (b) Illustration of strong Li^+–S_x^{2-} bond networks disrupted from competing for electrostatic interactions between Li ions and Li salt anions. (Reprinted with permission from [140], 2020, American Chemical Society.)

mote uniform Li deposition and mitigate the shuttle of LiPSs (Fig. 6a) [147–150]. Inspired by $LiNO_3$, analogous derivatives containing N–O bond have been developed, such as cesium nitrate ($CsNO_3$) [151], lanthanum nitrate ($La(NO_3)_3$) [152], zirconium oxynitrate ($ZrO(NO_3)_2$) [153], potassium nitrate (KNO_3) [154], and 1-butyl-3-methylimidazolium nitrate ([BMIM][NO_3]) [155]. However, NO_3^- is a sacrificial additive and the SEI formed by NO_3^- cannot maintain stable in long-term cycling. When referring to a pouch cell, the uneven utilization of the Li anode is very severe and the consumption of $LiNO_3$ is accelerated [60]. However, a high concentration of $LiNO_3$ above 0.5 M brings little contribution to the stability of the Li anode and even detrimentally reacts with active S [156]. Further, NO_3^- is an oxidant, and when coupling with S element and carbon, there is a risk of explosion in a confined space if thermal runaway occurs. Therefore, safety issues for practical applications while employing NO_3^- containing additives should be evaluated.

Li_2S/Li_2S_2 is a common component in the SEI with low ionic conductivity (~10^{-5} S cm^{-1}) due to the chemical/electrochemical reaction between LiPSs and Li metal [53,63,74,157]. There is a synergetic effect between LiPSs and $LiNO_3$ to form a robust SEI [150,158,159]. Nevertheless, the properties of the SEI are strongly dependent on the concentration and species of LiPSs [160–162]. When the total S concentration is fixed at 0.10 M, Li_2S_5 enables a better cycle performance compared to other LiPS species with 1.0 wt.% $LiNO_3$ additive [160]. A too low or too high concentration of LiPSs still cannot suppress the formation of Li dendrites even with 5.0 wt.% $LiNO_3$ (Fig. 6b) [161]. In practical Li–S batteries, a high S loading (>5 mg cm^{-2}) and low E/S ratio (<3.0 μL mgs^{-1}) always trigger a high-concentration LiPS electrolyte. Therefore, whether LiPSs can contribute to anode protection under practical conditions through precise regulation requires further investigation.

Besides inorganic Li_2S/Li_2S_2, transition metal sulfides, such as SeS_2 [163], CuS/Cu_2S [164,165], and MoS_2 [166], are also applied. Inorganic sulfide-solid-electrolytes with high ionic conductivity (~10^{-3} S cm^{-1}) are also favorable for fast Li ion transport [167–169]. A protection layer consisting of Li_3PS_4 can block the side reactions between Li metal and high-order LiPSs and restrain the electrolyte decomposition [169]. However, it is hard to maintain integrity for the pretreated *in situ* SEI at a huge utilization of the Li anode under practical conditions. In addition to inorganic sulfur-containing SEI, organosulfur-containing components are beneficial to improve the elasticity of SEI [170,171]. An inorganic/organic hybrid SEI is self-formed by adding poly(sulfur-ran dom-1,3-diisopropenylbenzene, PSD) into the electrolyte

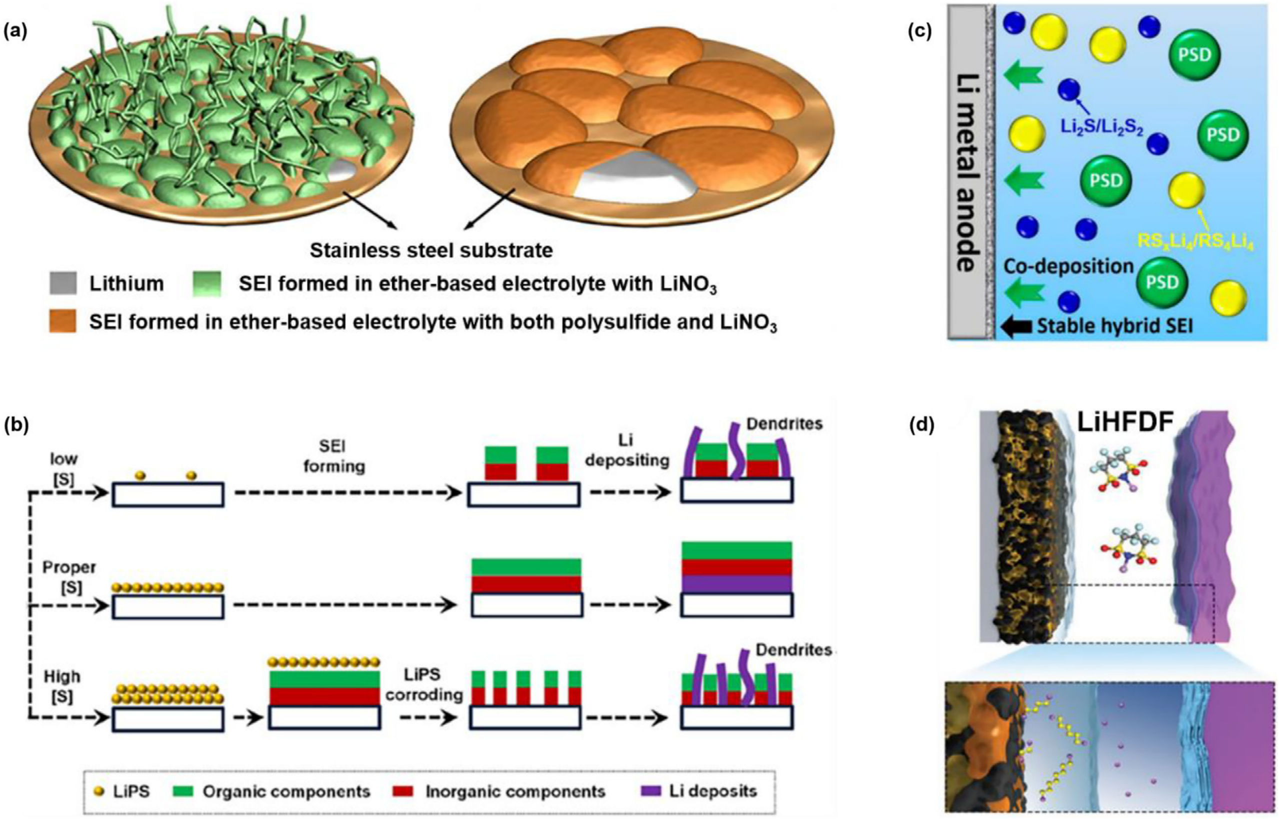

FIGURE 6

In situ SEI to protect the Li metal anode in Li–S batteries. (a) Schematic of the morphologies of Li deposited on the substrate in different electrolytes.[150] (b) The role of LiPS concentration on SEI evolution and Li deposition. (Reprinted with permission from [161], 2016, Elsevier.) (c) Self-formation of a stable hybrid SEI layer composed of Li organosulfides/organopolysulfides – Li_2S/Li_2S_2 using PSD as an electrolyte additive. (Reprinted with permission from [171], 2018, American Chemical Society.) (d) Schematic of how LiHFDF suppresses Li dendrite growth and shuttle of LiPSs. (Reprinted with permission from [178], 2020, Wiley-VCH.)

(Fig. 6c) [171]. The planar backbone conformation and the π–π interaction of aromatic-based species can enhance the toughness and flexibility of SEI, enabling uniform Li plating/stripping and high Coulombic efficiency.

Lithium fluoride (LiF) is generally identified as an efficient SEI component for uniform Li ion diffusion and Li deposition in other Li metal batteries [172–175]. However, the role of LiF in SEI for Li metal anode protection in Li–S batteries is controversial. Some publications hold the opinion that LiF is a beneficial SEI component in Li–S batteries [176–178], yet the regulation strategies are restricted due to the incompatibility between LiPSs and fluorinated carbonate esters. Fluoride-containing salts are alternative sources of LiF to establish fluorinated interphase, such as lithium difluoro(oxalato) borate (LiDFOB) [179–181] and lithium 1,1,2,2,3,3-hexafluoropropane-1,3-disulfonimide (LiHFDF, Fig. 6d) [178]. However, the content, distribution, and morphology of LiF in SEI are directly dependent on the fluorine sources. LiF formed by the decomposition of LiTFSI is limited in the routine electrolyte, which implies that LiF may not be the most important component in SEI in Li–S batteries [150]. Lithium bis(fluorosulfonyl)imide (LiFSI) is likely to be decomposed to form LiF in SEI compared to stable LiTFSI, while the LiFSI-induced SEI is too loose to shield the corrosive LiPSs as reported [182]. Therefore, the fundamental understanding of the functions of LiF in SEI is still insufficient, let alone its applications in practical batteries.

Artificial coating

An ideal artificial coating on the Li metal anode in Li–S batteries is expected to repulse the corrosion of LiPSs besides the necessary requirements of a single Li ion transport, a relief of volume change of Li metal, and enough flexibility and strength. The inherent stability of artificial coating in the presence of LiPSs is an important and basic requirement. Various inorganic/organic composite coatings, such as polyvinylidene fluoride (PVDF)-graphitic carbon nitride ($g\text{-}C_3N_4$) [183], PVDF-$Li_{1.5}Al_{0.5}Ge_{1.5}(PO_4)_3$ (Fig. 7a) [184], and Nafion-Li_xSiS_y [185], are employed to withstand the corrosive LiPSs. Moreover, the interactions between artificial coating and LiPSs can be regulated. The specific polar functional groups can repel LiPSs through electrostatic repulsion which is widely realized in separator modification [24,25,186]. Therefore, some functional groups on the outer surface of the artificial SEI may have distinctive interactions with LiPSs, thus regulating the adsorption and corrosion behaviors of LiPSs as polysulfiphobic sites. For example, Nafion has a good stability to resist the corrosion of LiPSs and repel LiPSs through $-SO_3^-$ group [187–189]. 1-decylphosphonic acid (DPA) can construct a robust interfacial film with abundant

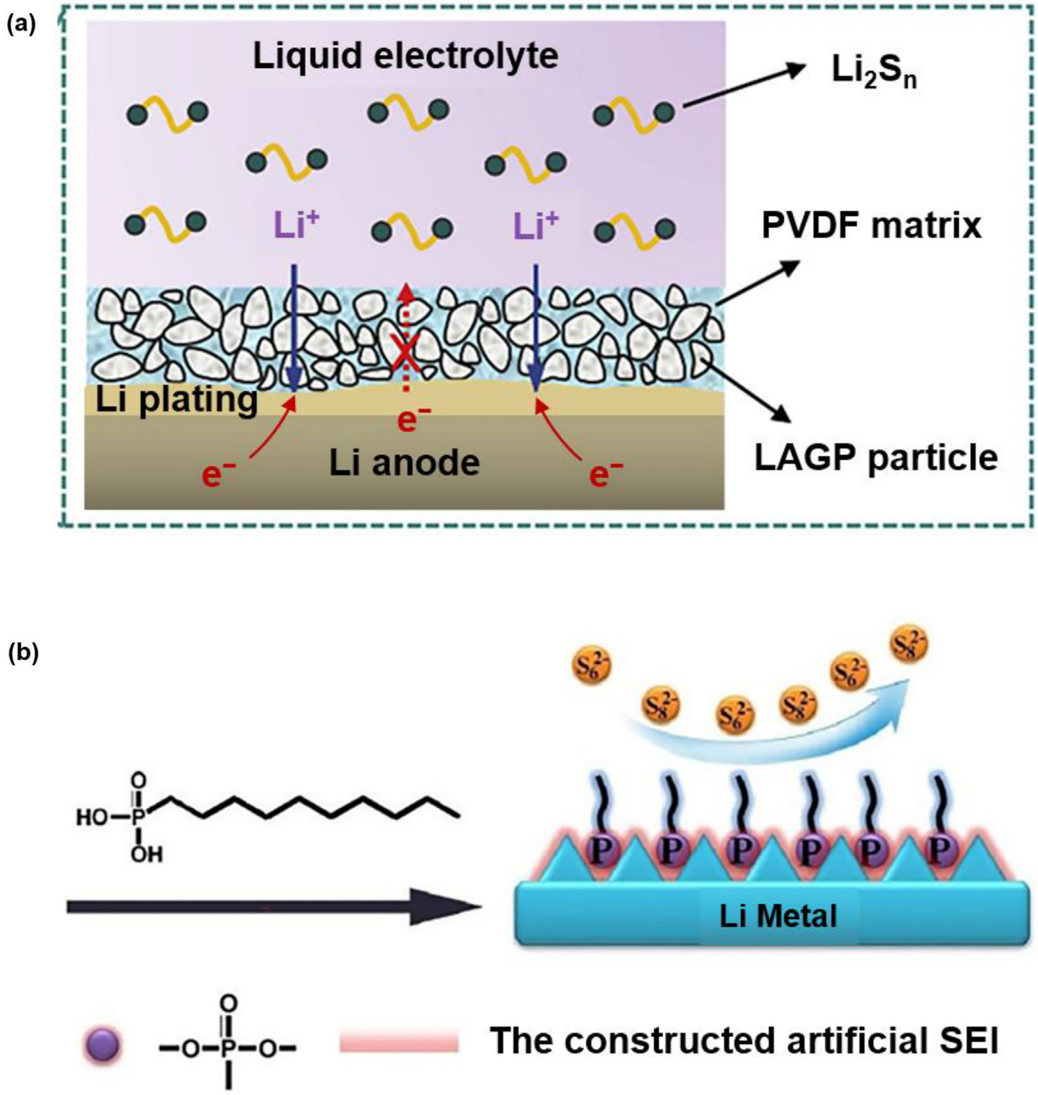

FIGURE 7

Artificial SEI to protect the Li metal anode in Li–S batteries. (a) Schematic of Li deposition behaviors with a PVDF-$Li_{1.5}Al_{0.5}Ge_{1.5}(PO_4)_3$ composite protective layer. (Reprinted with permission from [184], 2018, Elsevier.) (b) Schematic of the design and effect of Li decylphosphonate layer on the Li surface during repeated cycling. (Reprinted with permission from [190], 2018, American Chemical Society.)

decylphosphonate groups, which repulses LiPSs due to a low affinity with soluble LiPSs (Fig. 7b) [190].

When referring to the practical applications of artificial coating in Li–S batteries, several issues should be taken into consideration. Firstly, an artificial SEI is prepared before battery assembly and is irreparable. Secondly, more than 25 μm Li (>5 mAh cm^{-2}) will be utilized during each stripping or plating in a battery of 500 Wh kg^{-1}, and hence the artificial coating may lose intimate contact with the Li metal anode, especially with the accumulation of a dead Li layer between the artificial SEI and active Li after cycles. Thirdly, the increased interfacial resistance induced by the extrinsic artificial coating is a drawback. Finally, the spatial uniformity of the coating on the large anode is also an issue for the mechanical equipment in material preparation.

Modification of bulk Li

Improving the stability of bulk Li metal is an effective way to enhance the tolerance of the Li anode in LiPS electrolyte. Alloy can combine the traits of different types of metal. Various elements (B, Al, Si, Sn, *etc.*) have been alloyed with Li to improve the comprehensive properties, such as facilitating ion/atom conduction, relieving volume expansion of Li metal, and reducing local current density [191–193]. In Li–S batteries, the resistance of Li alloy to LiPS corrosion is an additional and necessary requirement.

The chemical stability of Li alloy is higher than that of pure Li metal partially due to the lattice reassortment and the increased electrochemical potential. Li–B alloy (Li_7B_6) with high electrochemical potential (>0.4 V *vs.* Li/Li^+) can increase the chemical stability toward the electrolyte [194]. A high conductivity (1.43×10^3 S cm^{-1}) and fast Li ion diffusivity restricts Li dendrites and reduces interfacial impedance [194–197]. Li–Al alloy (Li_9Al_4, ~0.3 V *vs.* Li/Li^+) possesses low reactive activity with LiPSs due to a strong combination between Li and Al, a low propensity of adatom clusters, and high surface diffusion barriers [198,199]. The formed SEI on the Li–Al alloy surface is also robust with the shallow distribution of Li_2S compared to the pure Li anode, favoring a homogeneous Li deposition (Fig. 8a) [200]. Al matrix with high Vickers hardness can further enhance uniform lithiation and unidirectional volume-strain circumvention [201]. The structure remains stable without deformation by local strain. Li–Mg alloy, with a theoretical specific capacity of 3151 mAh g^{-1} and an electrode potential near 0 V *vs*. Li/Li^+, exhibits high stability in Li–S batteries (Fig. 8b) [202]. Li–Mg alloy is resistant to the corrosion of LiPSs with a uniform passivation film on the alloy surface [202]. Li–Mg alloy maintains a solid solution state with a *bcc* β-phase during the range of Li content from 30 to 100 at.%, which reduces the barrier of Li nucleation [203]. The Li-poor alloy after delithiation acts as a mixed electron and Li ion conductive matrix to keep the structural integrity, indirectly inhibiting the exposure and propagation of Li dendrites in electrolyte [202].

In addition to the change of the properties of bulk Li metal, the modification of Li metal surface by alloy layer is also convenient to reconcile the high specific capacity of Li metal and the stability of alloy. Some heavy metals, such as Sn [204,205], Sb [206], and Bi [207], which are against high energy density, can be reutilized as an alloy layer on Li anode. A nanometer Sn layer (~250 nm) coating on the Li surface can form a Li_5Sn_2 alloy to regulate the fast Li ion transport and inhibit the shuttle of LiPSs (Fig. 8c) [204]. However, once the alloy layer is destroyed by Li dendrites or drastic volume change during repeated cycling, it is impossible to self-repair. Moreover, the alloy layer is usually coupled with other components (such as LiF and organic species) to protect Li metal [207,208].

Conclusions and outlook

Soluble LiPSs are inevitable in Li–S batteries based on the dissolution–precipitation mechanism of the S cathode. The temporal and spatial change of LiPSs results in a dynamic electrolyte. LiPSs can react with and corrode Li anode. The LiPSs are also involved in the formation and evolution of SEI. In a practical Li–S battery with a limited Li anode, a high loading S cathode,

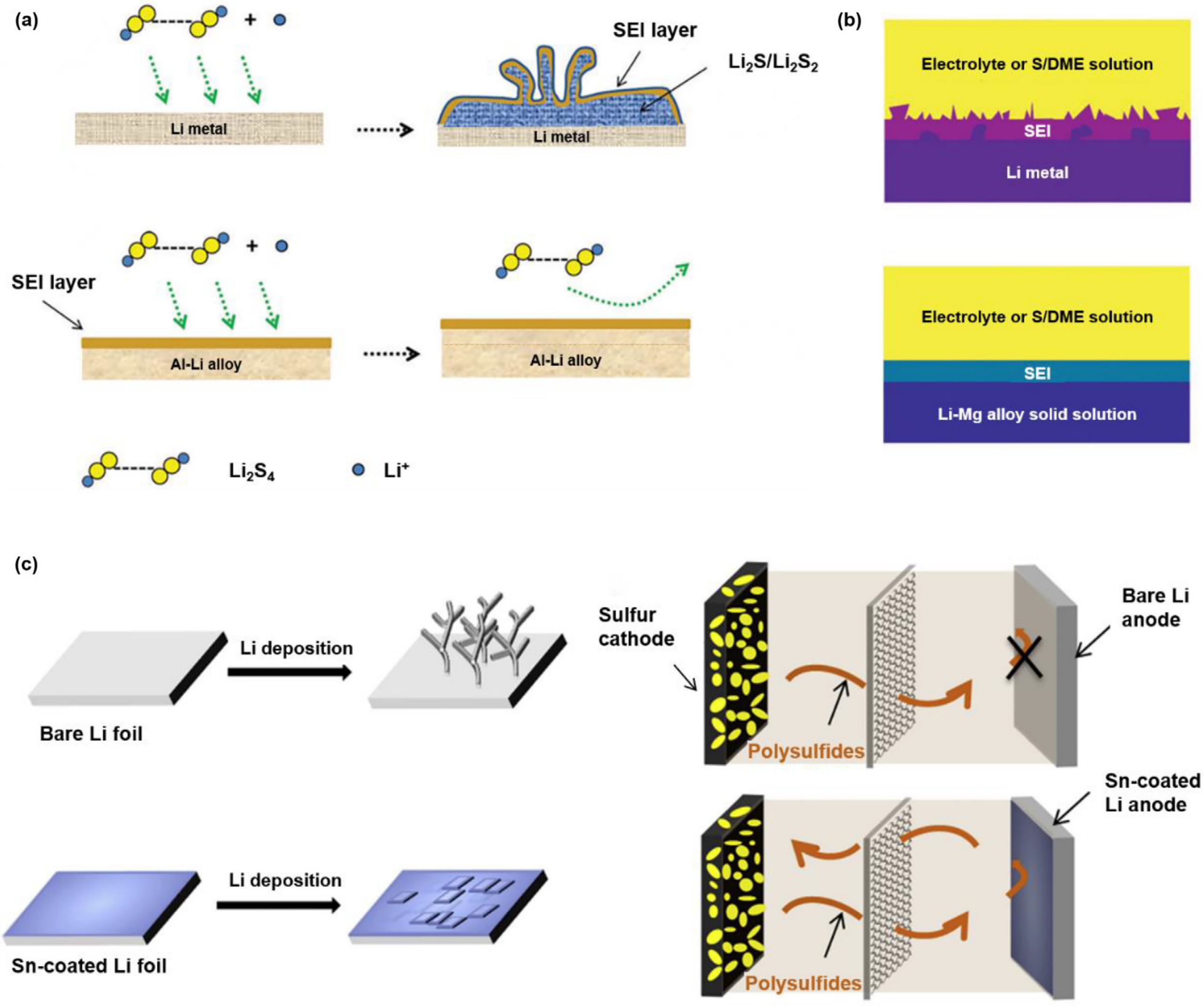

FIGURE 8

Reinforcement of bulk Li through the Li alloy anode or alloy interphase. (a) The illustration of interface stability of Li–Al alloy and Li metal in LiPS solution. (Reprinted with permission from [200], 2018, The Royal Society of Chemistry.) (b) Comparison of surface morphology evolutions between Li and Li–Mg alloy under different conditions. (Reprinted with permission from [202], 2019, Wiley-VCH.) (c) Schematic of Li deposition and LiPS shuttle behaviors on bare Li foil and Sn-coated Li foil. (Reprinted with permission from [204], 2020, Elsevier.)

and lean electrolyte, the Li metal anode is a bottleneck. Constructing a stable Li anode in the presence of LiPSs is a primary requirement for Li–S batteries. Preliminary efforts have been devoted to a stable Li metal anode, such as suppressing LiPS dissolution by decreasing free solvents and employing solvents with low polarity, decreasing the reactivity of LiPSs through interactions between cations and anions, and the regulation of SEI or bulk Li. However, both a fundamental understanding and practical exploration of the Li metal anode in Li–S batteries are in its infancy and more investigation is urgently required.

1) The fundamental understanding of LiPSs. The properties of LiPSs, that is, the dissolution state, dissociation ability, solvation features, diffusion coefficient, electric mobility, and electrochemical activity, as well as the features of LiPS electrolyte without other Li salts, such as ionic conductivity, viscosity, transfer number, and wettability, should be disclosed. In a real Li–S battery, the concentration and types of soluble LiPSs in electrolyte are dynamic during discharge/charge with complex electrochemical and chemical conversion, which is vital but unclear presently. The dilute solution of LiPSs is a preliminary platform to acquire basic physical, chemical, and electrochemical properties of LiPSs. The high-concentration LiPS solution (>4 M [S]) needs to be investigated to match the practical conditions of Li–S batteries with a high S loading, a low E/S ratio, and a limited Li metal anode.
2) The electrolyte structure in Li–S batteries. Generally, there is at least one Li salt in the electrolyte in a real battery, such as LiTFSI. Both Li salts and LiPSs contribute to the Li ions which can be solvated. If the Li ions are dissociated totally from LiPSs, the concentration of Li ions and the corresponding solvation of Li ions in electrolyte changes dynamically, especially under practical conditions. The anions, such as $TFSI^-$ and $S_x{}^{2-}$, can be involved in the solvation sheaths of Li ions. If Li ions are partially or barely dissociated from LiPSs but LiPSs are dissolved, especially at a low E/S ratio, two types of Li ions may coexist in an electrolyte. One is the dissociated Li ion from Li salts or LiPSs, and the other is undissociated Li ion in LiPSs. The dissociation of Li ions from LiPSs is impacted by the concentration and types of $S_x{}^{2-}$, Li salts, additives, and solvents in electrolyte. The structure of the undissociated LiPSs resembles the structure of CIP or AGG in highly concentrated electrolyte where the anions or the polysulfide chain of LiPSs are involved in the solvation sheath of Li ions and interact with solvent molecules through Van der Waals forces. If LiPSs aggregate into a cluster, solvents may interact with the LiPS cluster by a large sheath around the LiPS cluster. The solvation structure of both polysulfides and Li ions can be reflected by electrolyte properties, such as ionic conductivity, viscosity, transfer number, and wettability.
3) The SEI and Li metal while confronting LiPSs. The effect of LiPSs on the SEI is the foundation of further rational design. Participation in the formation of an SEI and the corrosion on the formed SEI are the main aspects in investigating the effect of LiPSs on the SEI. Furthermore, the properties of the SEI directly impact the following behaviors of Li deposition. The corrosion of LiPSs on Li is also of importance. To decrease the disturbance of LiPSs on the SEI, regulating the reactivity of LiPSs and constructing an SEI which can repel LiPSs are promising strategies. Further, the common requirements of an SEI, such as uniformity, rapid ion transport, and mechanical strength, are still necessary.
4) The design of the electrolyte. The routine electrolyte is 1.0 M LiTFSI in DOL/DME (1:1, by vol.) with various amounts of $LiNO_3$. The performance of the routine electrolyte under practical conditions, especially in pouch cells, is unsatisfactory. Novel electrolyte formulations are highly in demand. While considering the demand for high energy density, the electrolyte should keep a balance among the normal redox reaction of the S cathode, the suitable features of the electrolyte, and the stability of the Li metal anode. Li salts, solvents, and additives can be updated and adjusted to promote the practical applications.
5) Negative/positive ratio. Limited Li with a low negative/positive (N/P < 2) ratio is required in practical Li–S batteries with high energy density more than 500 Wh kg^{-1}. Moreover, a large amount of Li (>5 mAh cm^{-2}) participates in each stripping or plating process. As a comparison, N/P ratio is generally over 30 with a small amount of Li (<2 mAh cm^{-2}) engaging in each cycle under mild conditions. Limited Li under a low N/P ratio can be rapidly depleted and transformed into dead Li due to the low Coulombic efficiency of irregular and loose Li deposition, which also increases polarization and leads to short lifespan of batteries. Therefore, specific strategies to enhance the uniformity of Li deposition and increase the Coulombic efficiency of Li anode under a low N/P ratio are vital to extend the lifespan of Li–S batteries.
6) Specific and scientific method to assess the strategies of Li anode protection. Li | Li, Li | Cu, and Li | S battery configurations are widely used now. In a Li | Li symmetrical cell, the effect of LiPSs on the Li metal anode can be evaluated alone, instead of coupling with the complicated conversion of LiPSs at the S/C cathode in full batteries. It is demonstrated that LiPSs corrode Cu foil in a Li | Cu cell [209]. Therefore, conclusions conducted from battery configurations involving electrodes which are easily corroded by LiPSs should be treated with caution. With regard to testing conditions, a battery with a low loading S cathode (<2.0 mg cm^{-2}), a high E/S ratio (>10.0 μL mgs^{-1}), and a thick Li anode (>500 μm) cannot realistically reflect the effectiveness of the anode protection strategies due to the highly excess Li and electrolyte. Tests should preferably be carried out under conditions as close to the practical circumstances of high-energy-density Li–S batteries. A battery with a high loading S cathode (>5.0 mg cm^{-2}), a low E/S ratio (<3.0 μL mgs^{-1}), and a thin Li anode (<50 μm) is recommended in coin or pouch cells. The E/S ratio in a coin cell can be extended to 5.0 μL mgs^{-1} due to the existence of useless space inside.
7) Advanced characterizations and simulations. *In situ* or *ex situ* characterization tools, such as cryogenic electron microscopy, electrochemical quartz crystal microbalance,

and atomic force microscope, are required for a precise understanding of electrolyte, SEI, and Li ion/atom transport behaviors. Precise characterizations through X-ray absorption spectroscopy, Raman spectroscopy, nuclear magnetic resonance spectroscopy, ultraviolet–visible light spectroscopy, electron paramagnetic resonance, and so on, are also necessary to provide a clear understanding of LiPSs, including thermodynamic stable states, kinetic conversion pathways, solvation structure, chemical diffusion, and electromigration, especially at a low E/S ratio. Theoretical modeling, such as ab initio calculation, molecular dynamics, and phase field theory, is encouraged to be jointed to reveal the chemical structure of LiPSs, the solvation of LiPSs, SEI evolution, and Li plating/stripping behaviors. The combination of experiment and simulation can accelerate the progress of fundamental understanding and practical applications.

Groundbreaking technology requires time to develop. Such is the case with the practical application of the Li metal anode in Li–S batteries. Intensive attention should be paid to the fundamental understanding of the Li metal anode in LiPS electrolyte. Specific strategies for anode protection are required based on systematic understanding. Moreover, it is essential to verify the effectiveness of strategies under practical conditions after they have been validated in a proof-of-concept. The dramatic changes that LiPSs bring to the whole of battery systems should be considered cautiously in pouch cells. Persistent investigations on the Li metal anode in Li–S batteries will also shed fresh light on other advanced Li metal batteries for energy storage scenarios.

Conflict of interest

The authors have no conflict of interest.

CRediT authorship contribution statement

Li-Peng Hou: Conceptualization, Writing - review & editing. **Xue-Qiang Zhang:** Conceptualization, Writing - review & editing. **Bo-Quan Li:** Writing - review & editing, Visualization. **Qiang Zhang:** Conceptualization, Resources, Supervision, Funding acquisition, Project administration.

Acknowledgments

This work was supported by the National Natural Science Foundation of China (21825501 and U1801257), National Key Research and Development Program (2016YFA0202500), Scientific and Technological Key Project of Shanxi Province (20191102003), and the Tsinghua University Initiative Scientific Research Program.

References

[1] J.M. Tarascon, M. Armand, Nature 414 (2001) 359–367.
[2] B. Liu et al., Joule 2 (2018) 833–845.
[3] P.G. Bruce et al., Nat. Mater. 11 (2012) 19–29.
[4] G. Li et al., Chem 4 (2018) 3–7.
[5] D. Herbert, J. Ulam, U.S. Patent (1962) 3043896..
[6] J.L. Wang et al., Electrochem. Commun. 4 (2002) 499–502.
[7] J. Wang et al., Adv. Mater. 14 (2002) 963–965.
[8] X. Ji, L.F. Nazar, J. Mater. Chem. 20 (2010) 9821–9826.
[9] X. Ji et al., Nat. Mater. 8 (2009) 500–506.
[10] S.H. Chung, A. Manthiram, Adv. Mater. 31 (2019) 1901125.
[11] M. Zhao et al., Angew. Chem. Int. Ed. 59 (2020) 12636–12652.
[12] A. Bhargav et al., Joule 4 (2020) 285–291.
[13] S. Dörfler et al., Joule 4 (2020) 539–554.
[14] X. Zhang et al., Energy Environ. Sci. 13 (2020) 1076–1095.
[15] Q. Pang et al., Nat. Energy 1 (2016) 16132.
[16] Y.Z. Song et al., Adv. Energy Mater. 10 (2020) 1901075.
[17] X. Hong et al., J. Energy Chem. 42 (2020) 144–168.
[18] M. Zhang et al., Adv. Energy Mater. 10 (2020) 1903008.
[19] A. Manthiram et al., Chem. Rev. 114 (2014) 11751–11787.
[20] R. Steudel, T. Chivers, Chem. Soc. Rev. 48 (2019) 3279–3319.
[21] G. Li et al., Adv. Mater. 30 (2018) 1705590.
[22] C. Yan et al., Trends Chem. 1 (2019) 693–704.
[23] Y. Zhao et al., Adv. Mater. 31 (2019) 1806532.
[24] X. Li, X. Sun, Adv. Funct. Mater. 28 (2018) 1801323.
[25] L. Fan et al., Joule 3 (2019) 361–386.
[26] K. Mizushima et al., Mater. Res. Bull. 15 (1980) 783–789.
[27] K. Mizushima et al., Solid State Ionics 3–4 (1981) 171–174.
[28] M.M. Thackeray et al., Mater. Res. Bull. 19 (1984) 179–187.
[29] A.K. Padhi et al., J. Electrochem. Soc. 144 (1997) 1188–1194.
[30] N. Yabuuchi, T. Ohzuku, J. Power Sources 119 (2003) 171–174.
[31] I. Belharouak et al., J. Power Sources 123 (2003) 247–252.
[32] Q. Zou, Y.-C. Lu, J. Phys. Chem. Lett. 7 (2016) 1518–1525.
[33] M. Vijayakumar et al., Phys. Chem. Chem. Phys. 16 (2014) 10923–10932.
[34] M. Cuisinier et al., Adv. Energy Mater. 5 (2015) 1401801.
[35] G. Zhang et al., Angew. Chem. Int. Ed. 57 (2018) 16732–16736.
[36] C. Barchasz et al., Anal. Chem. 84 (2012) 3973–3980.
[37] C. Barchasz et al., Electrochim. Acta 89 (2013) 737–743.
[38] C. Zhang et al., J. Phys. Chem. C 118 (2014) 17362–17373.
[39] J. Gao et al., J. Phys. Chem. C 115 (2011) 25132–25137.
[40] T. Yim et al., Electrochim. Acta 107 (2013) 454–460.
[41] F.Y. Fan et al., J. Electrochem. Soc. 163 (2016) A3111–A3116.
[42] R. Xu et al., Adv. Energy Mater. 3 (2013) 833–838.
[43] C. Park et al., J. Phys. Chem. C 123 (2019) 10167–10177.
[44] A. Gupta et al., Adv. Energy Mater. 9 (2018) 1803096.
[45] J.W. Dibden et al., Chem. Commun. 52 (2016) 12885–12888.
[46] C. Shen et al., Electrochim. Acta 248 (2017) 90–97.
[47] C. Shen et al., J. Power Sources 414 (2019) 412–419.
[48] F.Y. Fan, Y.-M. Chiang, J. Electrochem. Soc. 164 (2017) A917–A922.
[49] S. Zhang et al., Adv. Energy Mater. 5 (2015) 1500117.
[50] L. Wang et al., Adv. Funct. Mater. 28 (2018) 1800919.
[51] N.N. Rajput et al., Chem. Mater. 29 (2017) 3375–3379.
[52] A. Andersen et al., Chem. Mater. 31 (2019) 2308–2319.
[53] H. Yamin, E. Peled, J. Power Sources 9 (1983) 281–287.
[54] E. Peled et al., J. Electrochem. Soc. 133 (1989) C290.
[55] D. Zheng et al., ChemSusChem 9 (2016) 2348–2350.
[56] L.E. Camacho-Forero et al., J. Phys. Chem. C 119 (2015) 26828–26839.
[57] Y. Han et al., Mater. Res. Bull. 68 (2015) 160–165.
[58] W.-T. Xu et al., ChemSusChem 8 (2015) 2892–2901.
[59] O. Salihoglu, R. Demir-Cakan, J. Electrochem. Soc. 164 (2017) A2948–A2955.
[60] X.-B. Cheng et al., Energy Storage Mater. 6 (2017) 18–25.
[61] L. Kong et al., Energy Technol. 7 (2019) 1900111.
[62] S. Xiong et al., J. Power Sources 236 (2013) 181–187.
[63] J.R. Akridge et al., Solid State Ionics 175 (2004) 243–245.
[64] Y.V. Mikhaylik, J.R. Akridge, J. Electrochem. Soc. 151 (2004) A1969–A1976.
[65] G. Rong et al., Adv. Mater. 29 (2017) 1606187.
[66] Y. Zhang et al., ACS Energy Lett. 2 (2017) 2696–2705.
[67] X.-B. Cheng et al., Chem. Rev. 117 (2017) 10403–10473.
[68] A. Jozwiuk et al., Energy Environ. Sci. 9 (2016) 2603–2608.
[69] X. Chen et al., Energy Storage Mater. 8 (2017) 194–201.
[70] C. Weller et al., J. Electrochem. Soc. 164 (2017) A3766–A3771.
[71] J.B. Goodenough, Y. Kim, Chem. Mater. 22 (2010) 587–603.
[72] M.D. Tikekar et al., Nat. Energy 1 (2016) 16114.
[73] P. Bai et al., Energy Environ. Sci. 9 (2016) 3221–3229.
[74] Z. Liu et al., ACS Appl. Mater. Interfaces 8 (2016) 4700–4708.
[75] R. Yemini et al., J. Electrochem. Soc. 166 (2019) A3098–A3101.
[76] F. Huang et al., J. Energy Chem. 49 (2020) 257–261.
[77] H. Liu et al., Adv. Energy Mater. 9 (2019) 1902254.
[78] D. Koo et al., Chem. Commun. 55 (2019) 9637–9640.
[79] M.I. Nandasiri et al., Chem. Mater. 29 (2017) 4728–4737.
[80] H. Wang et al., Adv. Funct. Mater. 28 (2018) 1707520.
[81] T.-Z. Hou et al., Angew. Chem. Int. Ed. 58 (2017) 8178–8182.
[82] L. Kong et al., Adv. Energy Mater. 8 (2018) 1800849.

[83] G. Li et al., Nat. Commun. 9 (2018) 705.
[84] H. Al Salem et al., J. Am. Chem. Soc. 137 (2015) 11542–11545.
[85] Z. Yuan et al., Nano Lett. 16 (2016) 519–527.
[86] M. Zhao et al., Angew. Chem. Int. Ed. 59 (2020) 9011–9017.
[87] D. Zheng et al., ACS Appl. Mater. Interfaces 8 (2016) 10360–10366.
[88] D. Lin et al., Nat. Nanotechnol. 12 (2017) 194–206.
[89] H. Zhang et al., Angew. Chem. Int. Ed. 57 (2018) 15002–15027.
[90] T. Li et al., Joule 3 (2019) 2647–2661.
[91] X. Zhang et al., Chem. Soc. Rev. 49 (2020) 3040–3071.
[92] E.S. Shin et al., Chem. Commun. 49 (2013) 2004–2006.
[93] H. Kim et al., Adv. Energy Mater. 5 (2015) 1401792.
[94] J. Zheng et al., Nano Energy 50 (2018) 431–440.
[95] L. Suo et al., Nat. Commun. 4 (2013) 1481.
[96] Q. Pang et al., Nat. Energy 3 (2018) 783–791.
[97] K. Yoshida et al., J. Am. Chem. Soc. 133 (2011) 13121–13129.
[98] K. Dokko et al., J. Electrochem. Soc. 160 (2013) A1304–A1310.
[99] F. Wu et al., Nano Lett. 20 (2020) 5391–5399.
[100] R. Glaser et al., J. Electrochem. Soc. 167 (2020) 100512.
[101] K. Sun et al., ACS Appl. Energy Mater. 1 (2018) 2608–2618.
[102] C. Weller et al., Energy Technol. 7 (2019) 1900625.
[103] A. Shyamsunder et al., Angew. Chem. Int. Ed. 56 (2017) 6192–6197.
[104] X. Wang et al., J. Energy Chem. 41 (2020) 149–170.
[105] M. Shin et al., ACS Appl. Mater. Interfaces 9 (2017) 39357–39370.
[106] C.-C. Su et al., Angew. Chem. Int. Ed. 57 (2018) 12033–12036.
[107] C.-C. Su et al., Angew. Chem. Int. Ed. 58 (2019) 10591–10595.
[108] L. Cheng et al., ACS Energy Lett. 1 (2016) 503–509.
[109] W. Weng et al., Adv. Mater. 25 (2013) 1608–1615.
[110] N. Azimi et al., Electrochem. Commun. 37 (2013) 96–99.
[111] N. Azimi et al., ACS Appl. Mater. Interfaces 7 (2015) 9169–9177.
[112] N. Azimi et al., J. Electrochem. Soc. 162 (2015) A64–A68.
[113] M.L. Gordin et al., ACS Appl. Mater. Interfaces 6 (2014) 8006–8010.
[114] S. Chen et al., ACS Appl. Mater. Interfaces 9 (2017) 6959–6966.
[115] H. Lu et al., J. Electrochem. Soc. 162 (2015) A1460–A1465.
[116] M. Gao et al., J. Mater. Chem. A 5 (2017) 6725–6733.
[117] J. Zheng et al., Adv. Energy Mater. 9 (2019) 1803774.
[118] Y. Yamada et al., J. Am. Chem. Soc. 136 (2014) 5039–5046.
[119] M. Cuisinier et al., Energy Environ. Sci. 7 (2014) 2697–2705.
[120] C.-W. Lee et al., ACS Cent. Sci. 3 (2017) 605–613.
[121] A. Nakanishi et al., J. Phys. Chem. C 123 (2019) 14229–14238.
[122] M. Yanagi et al., J. Electrochem. Soc. 167 (2020) 070531.
[123] L.X. Yuan et al., Electrochem. Commun. 8 (2006) 610–614.
[124] J.H. Shin, E.J. Cairns, J. Electrochem. Soc. 155 (2008) A368–A373.
[125] M. Watanabe et al., Chem. Rev. 117 (2017) 7190–7239.
[126] M. Schmeisser et al., Chem. Eur. J. 18 (2012) 10969–10982.
[127] J.-W. Park et al., J. Phys. Chem. C 117 (2013) 20531–20541.
[128] M.Y. Lui et al., Chem. Sci. 2 (2011) 1491–1496.
[129] J.-W. Park et al., J. Phys. Chem. C 117 (2013) 4431–4440.
[130] R.G. Pearson, J. Am. Chem. Soc. 85 (1963) 3533–3539.
[131] S.S. Zhang, Electrochim. Acta 97 (2013) 226–230.
[132] Y. Chen et al., Adv. Funct. Mater. 28 (2018) 1704987.
[133] U. Pal et al., J. Phys. Chem. C 122 (2018) 14373–14382.
[134] S. Xiong et al., J. Power Sources 252 (2014) 150–155.
[135] H.K. Seo et al., Nano Lett. 20 (2020) 2080–2086.
[136] Q. Zou et al., J. Am. Chem. Soc. 140 (2018) 10740–10748.
[137] H. Pan et al., ACS Appl. Mater. Interfaces 9 (2017) 4290–4295.
[138] H. Pan et al., Adv. Funct. Mater. 28 (2018) 1707234.
[139] T. Yu et al., J. Mater. Chem. A 5 (2017) 9293–9298.
[140] A. Gupta et al., Chem. Mater. 32 (2020) 2070–2077.
[141] J. Chen et al., Adv. Energy Mater. 6 (2016) 1600160.
[142] K.S. Han et al., Chem. Mater. 29 (2017) 9023–9029.
[143] E. Peled, J. Electrochem. Soc. 126 (1979) 2047–2051.
[144] X.-Q. Zhang et al., Adv. Mater. Interfaces 5 (2018) 1701097.
[145] S.Y. Bai et al., Joule 2 (2018) 2117–2132.
[146] Y.V. Mikhaylik, U.S. Patent (2008) 7352680..
[147] D. Aurbach et al., J. Electrochem. Soc. 156 (2009) A694–A702.
[148] S.S. Zhang, Electrochim. Acta 70 (2012) 344–348.
[149] S. Xiong et al., J. Power Sources 246 (2014) 840–845.
[150] W. Li et al., Nat. Commun. 6 (2015) 7436.
[151] J.-S. Kim et al., ChemNanoMater 1 (2015) 240–245.
[152] S. Liu et al., ACS Appl. Mater. Interfaces 8 (2016) 7783–7789.
[153] J. Li et al., J. Power Sources 442 (2019) 227232.
[154] W. Jia et al., ACS Appl. Mater. Interfaces 8 (2016) 15399–15405.
[155] Y.-X. Yao et al., InfoMat 2 (2019) 379–388.
[156] Y. Ye et al., Energy Storage Mater. 16 (2019) 498–504.
[157] H. Yamin et al., J. Power Sources 14 (1985) 129–134.
[158] X.B. Cheng et al., Chem 2 (2017) 258–270.
[159] L. Zhang et al., Energy Storage Mater. 11 (2018) 24–29.
[160] C.-Z. Zhao et al., Energy Storage Mater. 3 (2016) 77–84.
[161] C. Yan et al., J. Power Sources 327 (2016) 212–220.
[162] X.-B. Cheng et al., Energy Storage Mater. 10 (2018) 199–205.
[163] F. Liu et al., Adv. Funct. Mater. 30 (2020) 2001607.
[164] C. Zu, A. Manthiram, J. Phys. Chem. Lett. 5 (2014) 2522–2527.
[165] L. Jia et al., ACS Appl. Mater. Interfaces 8 (2016) 30248–30255.
[166] E. Cha et al., Nat. Nanotechnol. 13 (2018) 337–344.
[167] Q. Pang et al., Joule 1 (2017) 871–886.
[168] Y. Lu et al., Energy Storage Mater. 11 (2018) 16–23.
[169] J. Liang et al., Adv. Mater. 30 (2018) 1804684.
[170] G. Li et al., Nat. Commun. 8 (2017) 850.
[171] G. Li et al., ACS Nano 12 (2018) 1500–1507.
[172] Y. Lu et al., Nat. Mater. 13 (2014) 961–969.
[173] X.-Q. Zhang et al., Angew. Chem. Int. Ed. 57 (2018) 5301–5305.
[174] S. Jurng et al., Energy Environ. Sci. 11 (2018) 2600–2608.
[175] M. He et al., Proc. Natl. Acad. Sci. USA 117 (2020) 73–79.
[176] D. Lin et al., Nano Lett. 17 (2017) 3731–3737.
[177] B. Tang et al., Small 16 (2020) 1905737.
[178] Y. Xiao et al., Adv. Energy Mater. 10 (2020) 1903937.
[179] F. Wu et al., ACS Appl. Mater. Interfaces 6 (2014) 15542–15549.
[180] N. Azimi et al., Electrochim. Acta 154 (2015) 205–210.
[181] F. Wu et al., J. Power Sources 296 (2015) 10–17.
[182] R. Cao et al., Adv. Funct. Mater. 26 (2016) 3059–3066.
[183] C. Xiong et al., J. Energy Storage 26 (2019) 101006.
[184] C. Sun et al., J. Power Sources 377 (2018) 36–43.
[185] Q. Jin et al., J. Mater. Chem. A 8 (2020) 8979–8988.
[186] S.Y. Bai et al., Nat. Energy 1 (2016) 16094.
[187] C. Shen et al., Nano Energy 19 (2016) 68–77.
[188] T.-Z. Zhuang et al., Small 12 (2016) 381–389.
[189] S. Jiang et al., Chem. Asian J. 13 (2018) 1379–1385.
[190] X. Shen et al., ACS Appl. Mater. Interfaces 10 (2018) 30058–30064.
[191] C.-M. Park et al., Chem. Soc. Rev. 39 (2010) 3115–3141.
[192] M.N. Obrovac, V.L. Chevrier, Chem. Rev. 114 (2014) 11444–11502.
[193] H. Liu et al., ACS Mater. Lett. 1 (2019) 217–229.
[194] B. Duan et al., ECS Electrochem. Lett. 2 (2013) A47–A51.
[195] D. Zhou et al., Electrochim. Acta 51 (2006) 5731–5737.
[196] X.-B. Cheng et al., Small 10 (2014) 4257–4263.
[197] X. Zhang et al., J. Mater. Chem. A 2 (2014) 11660–11665.
[198] M. S. Kim, et al., Sci. Adv. 5 (2019) eaax5587.
[199] A.V. Markevych et al., ECS Trans. 95 (2019) 9–17.
[200] J. Sun et al., Energy Environ. Sci. 11 (2018) 2509–2520.
[201] H. Li et al., Nat. Commun. 11 (2020) 1584.
[202] L.-L. Kong et al., Adv. Funct. Mater. 29 (2019) 1808756.
[203] A.A. Nayeb-Hashemi et al., Bull. Alloy Phase Diagrams 5 (1984) 365–374.
[204] S. Xia et al., Energy Storage Mater. 24 (2020) 329–335.
[205] C. Li et al., ACS Appl. Mater. Interfaces 11 (2019) 2479–2489.
[206] T. Chen et al., Chem. Mater. 31 (2019) 7565–7573.
[207] Y.X. Ren et al., Nat. Commun. 10 (2019) 3249.
[208] L. Ma et al., Chem. Mater. 29 (2017) 4181–4189.
[209] X. Zhang et al., Energy Storage Mater. 18 (2019) 199–204.